Influence of axionic fields on large scale structures

Hideo Kodama

@ ExDiP2010 2010.11.12

Probing the Ultimate Theory by Axion Cosmophysics

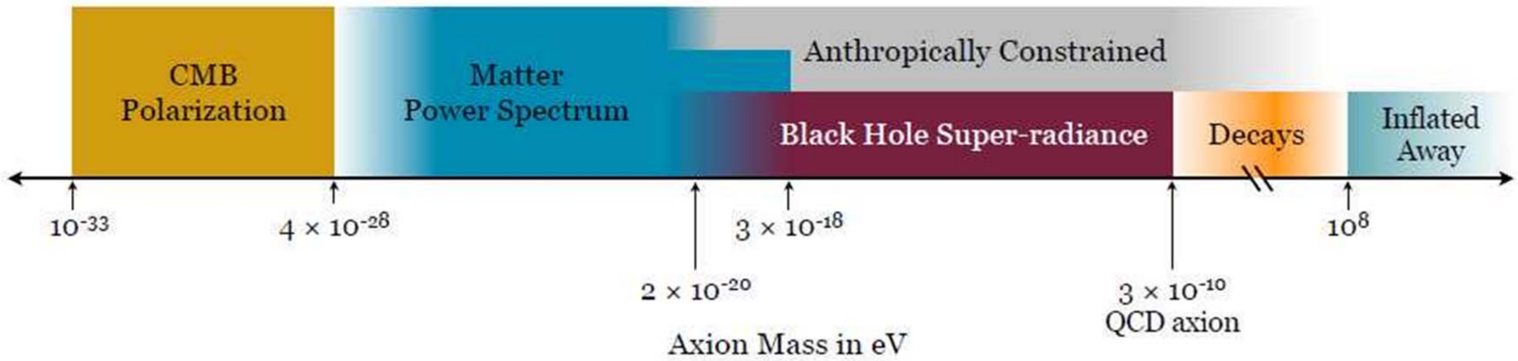

String theories predict the existence of superlight axionic moduli , which provoke various new cosmophysical phenomena.

- **CMB polarisation : Birefringence**

  [Carroll, Field, Jackiw 1990; Ni W-T 1977; Lu, Wang, Kamionkowski 1999]

- **Large scale structure : Power spectrum modification**

  [Hu W, Barkana R, Gruzinov A 2000; ADDKM 2009; Marsh, Ferreira 2010]

- **Black hole instability : BH bomb/axion siren**

  [Damour, Deruelle, Ruffini 1976; ADDKM 2009]

- **Anomalous UHE gamma : Penetration of the GZK type barrier of CMB**

Arvanitaki A, Dimopoulos S,Dubovsky S, Kaloper N, March-Russell, J: “String Axiverse” arXiv: 0905.4720

HOMOGENEOUS BACKGROUND

Behavior of a light coherent field

Field equation

$$\ddot{\phi} + 3H\dot{\phi} + m^2\phi = 0 \Rightarrow \quad (a^{3/2}\phi)^{\cdot\cdot} + \left(m^2 - \frac{3}{4}H^2 - \frac{3}{2}\frac{\ddot{a}}{a}\right)(a^{3/2}\phi) = 0$$

$$\rho_\phi = \frac{1}{2}\left(\dot{\phi}^2 + m^2\phi^2\right)$$

Basic behavior

– H $\gtrsim$ m/3: ➡ DE/Λ

$$\phi = \phi_0 + C\int_{t_0}^{t}\frac{dt}{a^3} \to \text{const}$$

– H $\lesssim$ m/3: ➡ dust-like matter

$$\phi = \frac{A}{(ma^3)^{1/2}}\sin\left(\int m\,dt + \text{const}\right)$$

$$\Rightarrow \quad \rho_\phi \approx \frac{mA^2}{2a^3} \approx \left(\frac{a(t_m)}{a}\right)^3 \frac{m}{m(t_m)}\rho_\phi(t_m)$$

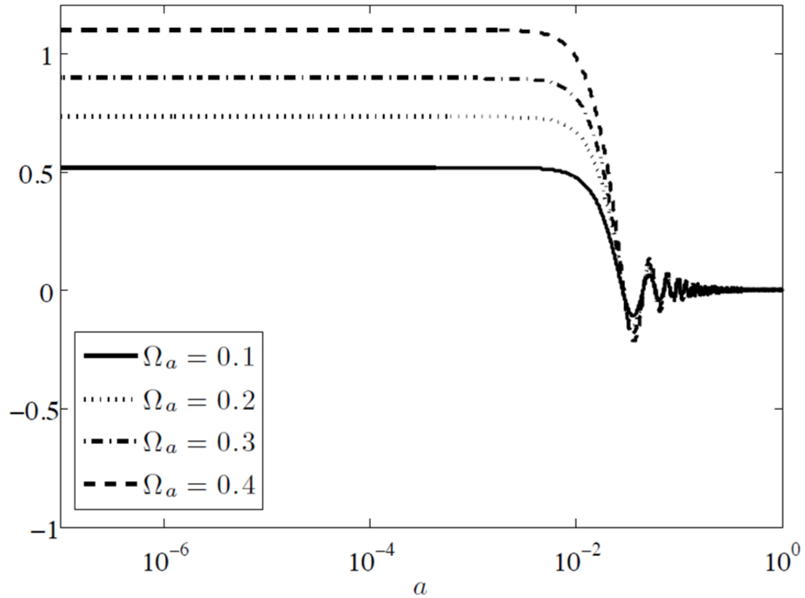

m/H_0 =10^3, Ω_Λ =0

Time Evolution of ρ_ϕ and the expansion rate

Axion field behaves as a cosmological constant in the early stage and as non-relativistic matter in the late stage.

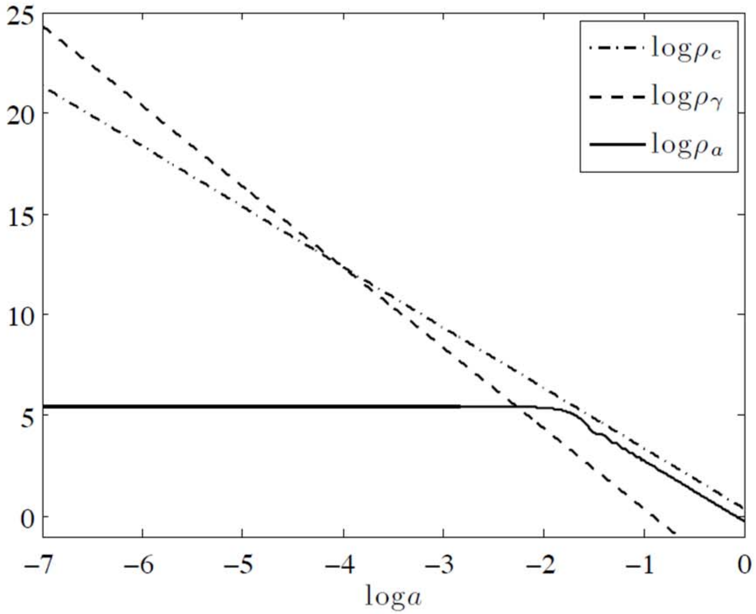

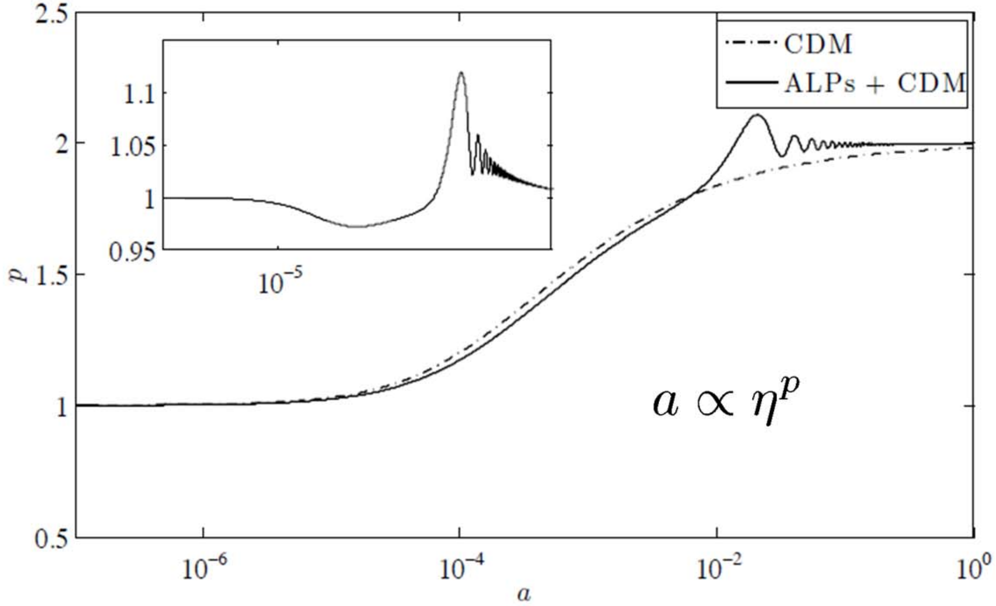

$$m/H_0 = 10^3, \quad \Omega_c = 0.8, \quad \Omega_\Lambda = 0$$

Marsh DJE, Ferreira PG: arXiv:1009.3501

Characteristic Mass Scales

- 3/m= Horizon size (=1/H)
  - Present $t=t_0$: $m=m_0=4.5\times 10^{-33}$ eV
  - CMB last scattering $t=t_{ls}$: $m=0.7\times 10^{-28}$ eV
  - H recombination $t=t_{rec}$: $m=m_{rec}=1.2\times 10^{-28}$ eV
  - Equidensity time $t=t_{eq}$: $m=m_{eq}=0.9\times 10^{-27}$ eV

- QCD axion $m \approx \Lambda_{QCD}^2/f_a$
  - $f_a=10^{16}$ GeV: $m \sim 10^{-9}$ eV
  - $f_a= 10^{12}$ GeV: $m \sim 10^{-5}$ eV

Cf. $m_a = 1\mathrm{eV} \times \left(\frac{6\times 10^6\,\mathrm{GeV}}{f_a}\right)$

Density Parameter

$m < 3H_0$

Dark Energy

$$\rho_\phi = \frac{1}{2} m^2 (\epsilon f_a)^2 \quad \Rightarrow \quad \Omega_\phi = \frac{3\epsilon^2}{2}\left(\frac{m}{3H_0}\right)^2 \left(\frac{f_a}{m_{\rm pl}}\right)^2 \lesssim \left(\frac{f_a}{m_{\rm pl}}\right)^2$$

$3H_0 < m$

$$\rho_\phi = m a_*^3 \times \frac{1}{2} m_* (\epsilon f_a)^2$$

Dark Matter

$3H_0 < m < 3H_{\rm eq}$

$$\Rightarrow \quad \Omega_\phi = \frac{3\epsilon^2}{2}\left(\frac{m}{m_*}\right)\left(\frac{a_*^3 H_*^2}{H_0^2}\right)\left(\frac{f_a}{m_{\rm pl}}\right)^2 \approx \left(\frac{f_a}{m_{\rm pl}}\right)^2$$

$3H_{\rm eq} < m$

$$\Rightarrow \quad \Omega_\phi \approx \frac{3\epsilon^2}{2}\left(\frac{m}{m_*}\right)\Omega_R^{3/4}\left(\frac{m}{3H_0}\right)^{1/2}\left(\frac{f_a}{m_{\rm pl}}\right)^2$$

$$\approx \left(\frac{m}{m_{\rm eq}}\right)^{1/2}\left(\frac{f_a}{m_{\rm pl}}\right)^2$$

Present Abundance

For 10^{-26}eV < m < 10^{-28} eV, the density parameter of the axion is (1-0.1) Ω_μ, if $f_a \sim m_{pl}$.

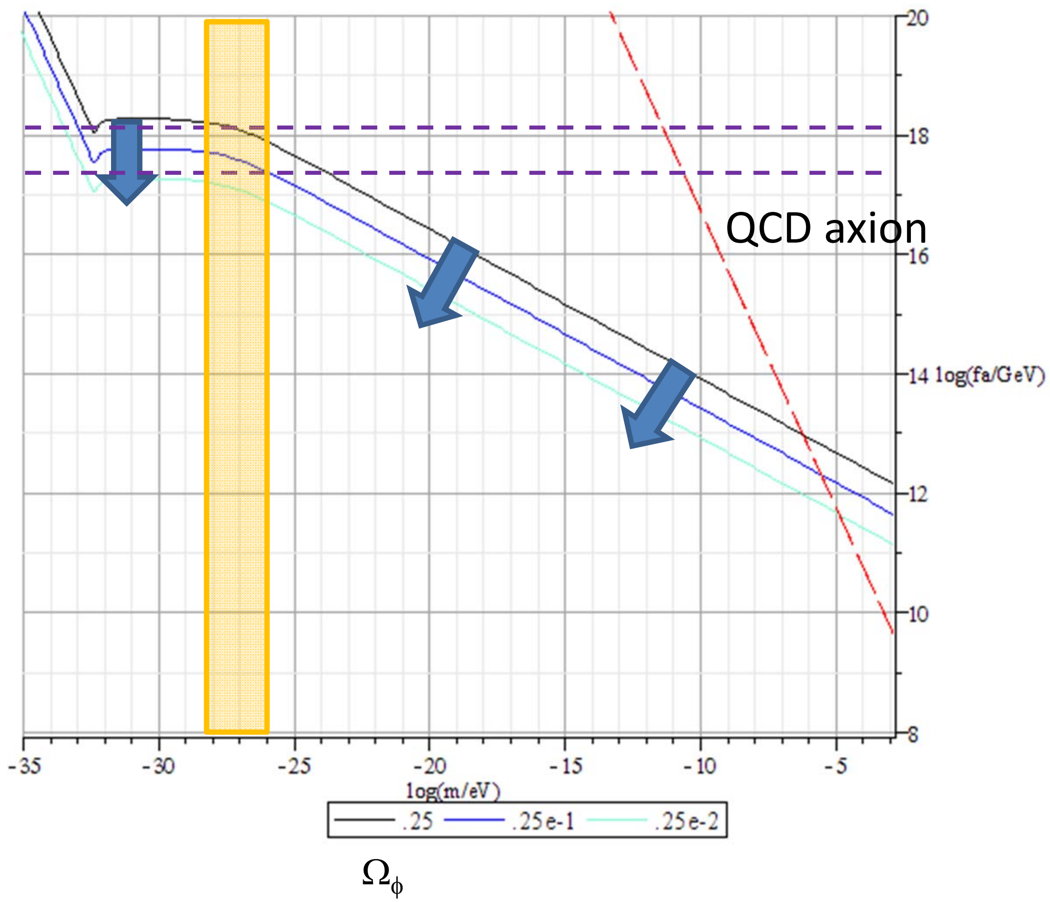

BOSONIC DARK MATTER

Fuzzy Cold Dark Matter

Wayne Hu, R Barkana, A Gruzinov: PRL85, 1158 (2000)

Newton Approximation in the Oscillatory Phase

$$\phi(t,x) = Ae^{-imt+\alpha} = \psi(t,x)e^{-imt}$$
$$ds^2 = -(1+2\Psi)dt^2 + (1-2\Psi)a^2dx^2$$

Assume $|\dot{\psi}| \ll m|\psi|,\ |\dot{\Psi}| \ll m$

$$i\left(\partial_t + \frac{3}{2}H\right)\psi \approx \left(-\frac{1}{2ma^2}\triangle + m\Psi\right)\psi$$

For $k \ll m$, non-relativistic fluid with

$$\rho = \frac{m^2}{2}|\psi|^2, \quad \rho v = i\frac{m}{4a}(\psi\nabla\psi^* - \psi^*\nabla\psi) \quad \Rightarrow \quad mv = \frac{k}{a}$$

Resolution of the Cusp/Substructure Problem

JEANS LENGTH

$$c_s \approx v = \frac{k}{am}$$

$$\Rightarrow \frac{k_J}{a} \approx \frac{\sqrt{G\rho}}{c_s} \approx \frac{amH}{k_J}$$

$$\Rightarrow L_J \approx \frac{a}{\sqrt{mH}}$$

Suppression of inhomogeneities
on scales smaller than

$$k \lesssim \frac{1}{2} k_{\mathrm{J,eq}} m_{22}^{-1/18} \simeq 4.5 m_{22}^{4/9} \mathrm{Mpc}^{-1}$$

The cusp/substructure problem in CDM can be resolved if the dark matter consists of scalar field of mass ~ 10^{-22} eV.

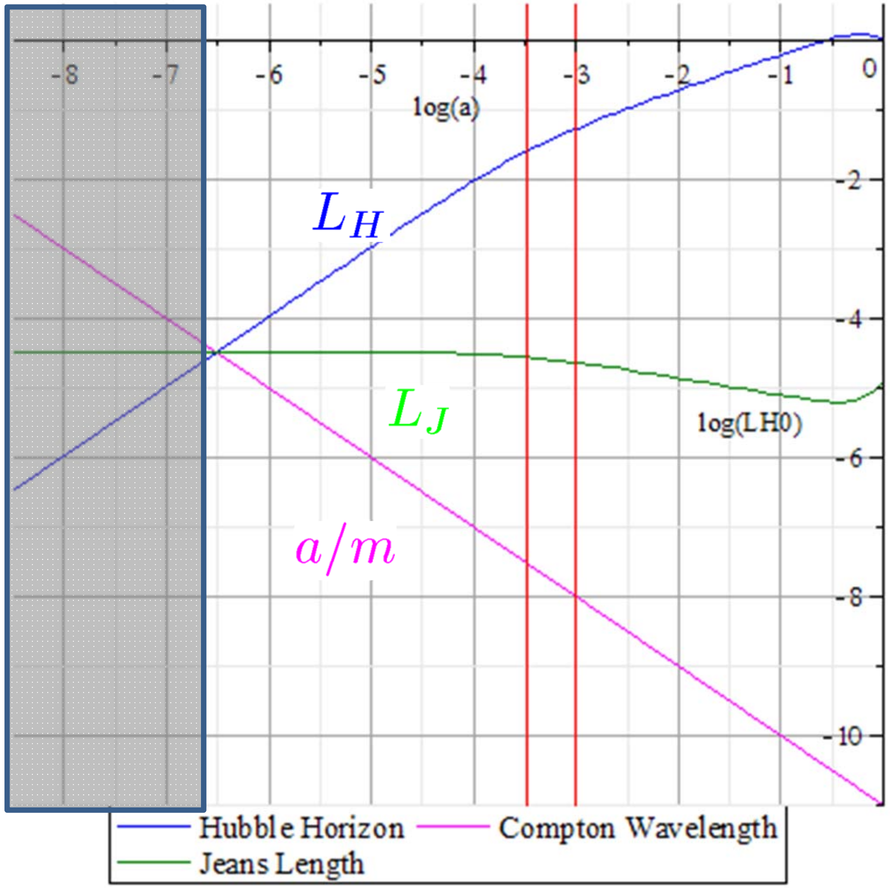

Influences on LSS

Behavior of Perturbations

$H > m$ frozen

$H < m$ & $k < k_J$ the same as the standard CDM

$H < m$ & $k > k_J$ damped oscillation

Spectral deformation

$$S := \frac{\Delta(\mathrm{CDM} + \mathrm{axion})}{\Delta(\mathrm{CDM})}$$

$k < k_m = aH$ at $H=m$ $S=1$

$k > k_{J,0} = k_J(t_0)$ $S=\mathrm{const} <1$

⇨ Step-like deformation!

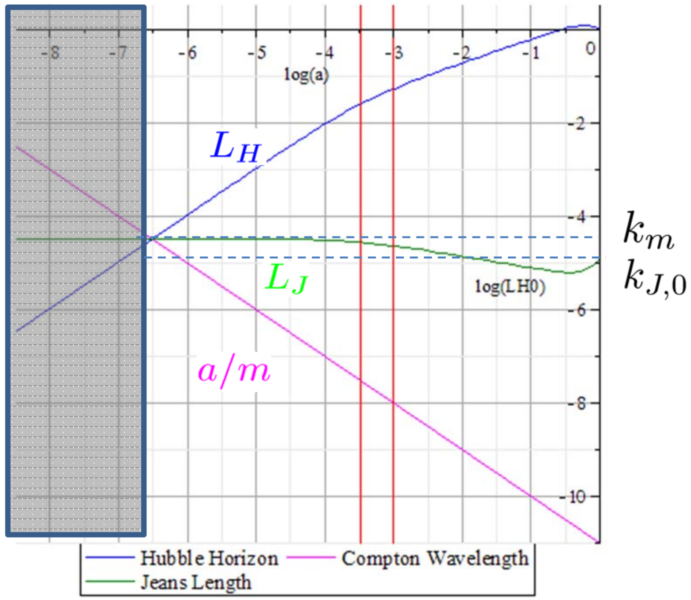

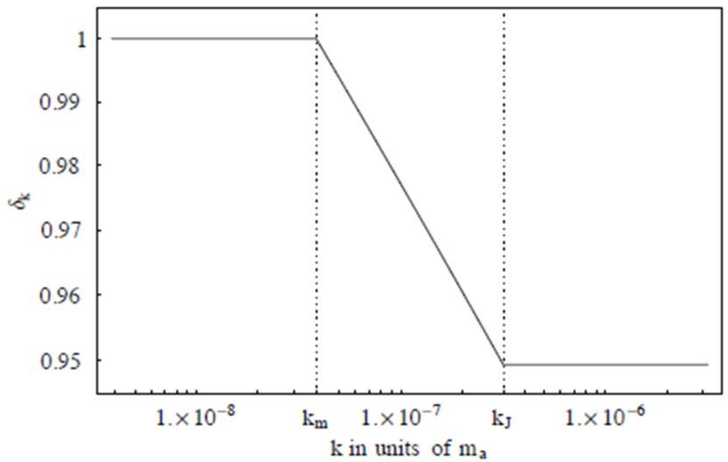

The characteristic scales depend on m

$m \simeq 10^{-22}\mathrm{eV}$

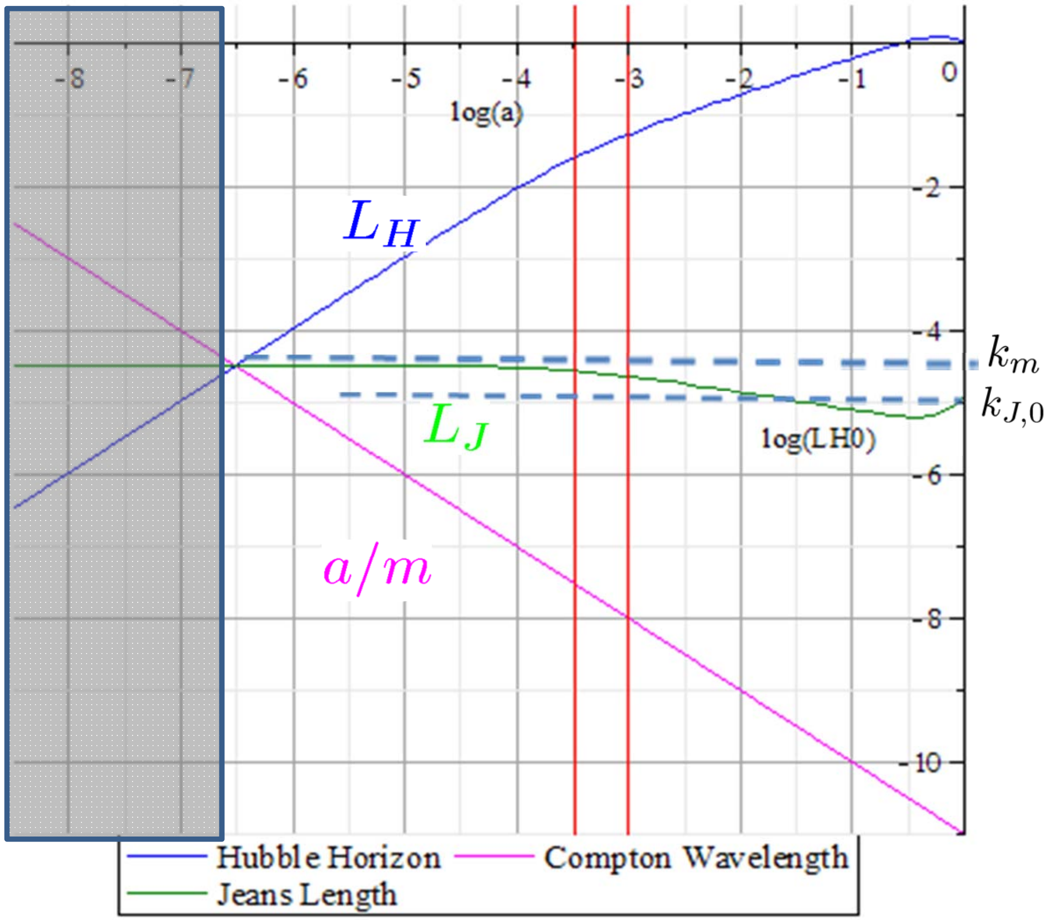

$m \simeq 10^{-27}\mathrm{eV}$

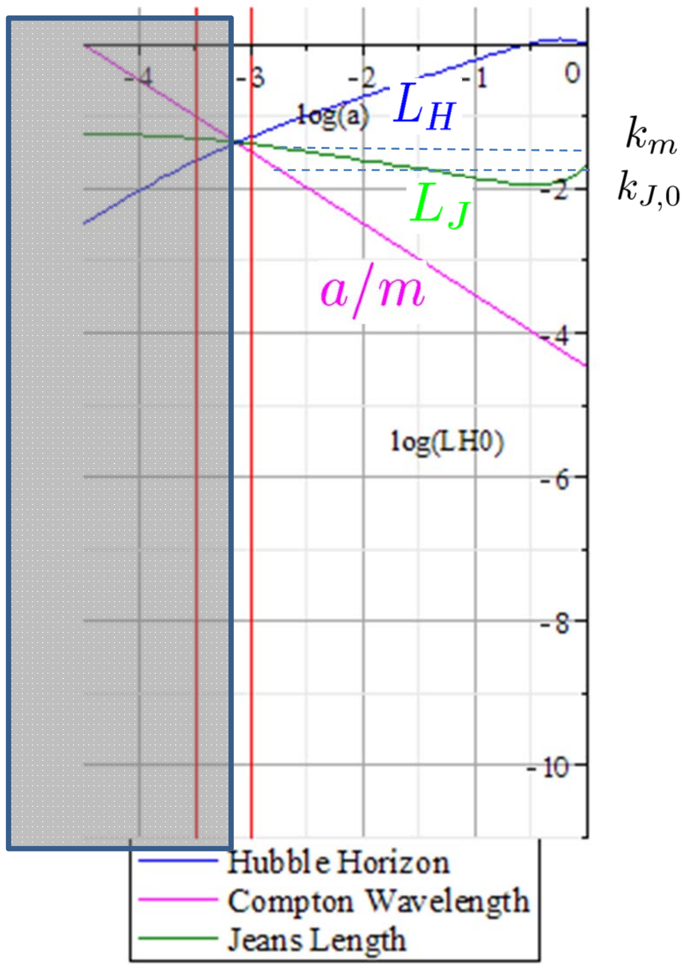

$$m > m_{\rm eq} \simeq 10^{-27}\,{\rm eV}$$

$$k_m \approx \left(\frac{m}{2\cdot 10^{-24}\,{\rm eV}}\right)^{1/2} {\rm Mpc}^{-1}$$

$$k_{J,o} \approx \left(\frac{m}{2\cdot 10^{-25}\,{\rm eV}}\right)^{1/2} {\rm Mpc}^{-1}$$

$$m < m_{\rm eq} \simeq 10^{-27}\,{\rm eV}$$

$$k_m \approx \left(\frac{m}{4\times 10^{-22}\,{\rm eV}}\right)^{1/3} {\rm Mpc}^{-1}$$

$$k_{J,o} \approx \left(\frac{m}{2\cdot 10^{-25}\,{\rm eV}}\right)^{1/2} {\rm Mpc}^{-1}$$

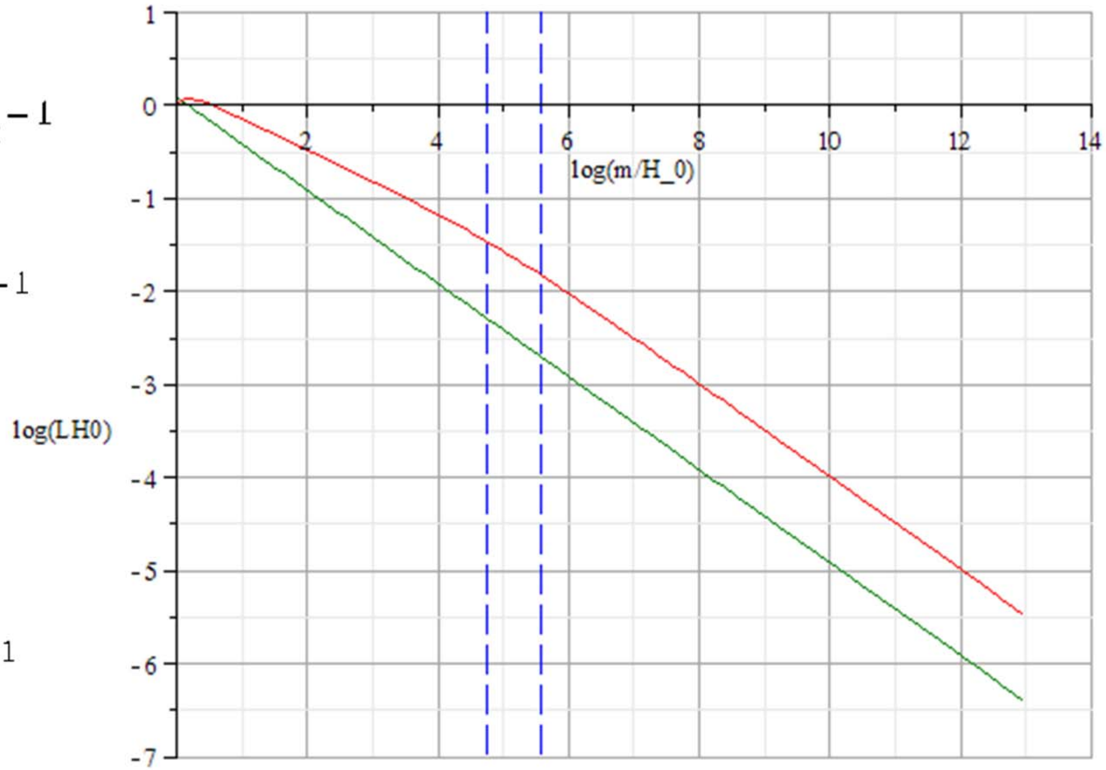

Cf. Axiverse Paper

- The suppression factor S is given by

$$S(z_J) \simeq \left(\frac{z_{\rm eq}+1}{z_J+1}\right)^{-3\Omega_a/5\Omega_m} \approx 1 - \frac{3\Omega_a}{5\Omega_m} \ln \frac{z_{\rm eq}+1}{z_J+1}$$

where

$$\frac{\Omega_a}{\Omega_m} \simeq \frac{f_a^2}{3m_{\rm pl}^2}\frac{1+z_m}{1+z_{\rm eq}}; \quad z_m \approx \frac{m^{1/2} z_{\rm eq}^{1/4}}{(3H_0)^{1/2}\Omega_m^{1/4}} \simeq z_{\rm eq}\left(\frac{m}{6\cdot 10^{-28}{\rm eV}}\right)^{1/2}$$

For $m \sim 10^{-22}$eV for which $k_J \sim 1$Mpc^{-1},

$$\frac{f_a^2}{3m_{\rm pl}^2} \sim 10^{-5} \Rightarrow \quad 1 - S \sim 4 \cdot 10^{-3}$$

- Observations
  - Current limits: Ly-α lines $\Rightarrow \Omega_a/\Omega_m \lesssim 0.1$ for k=(0.1−10)Mpc^{-1}, $z_o = 2 \sim 4$.
  - Future observations: BOSS (SDSSIII) and the 21cm line measurement will give much stronger limits/detections.

MASSIVE NEUTRINO

Influence of neutrino mass on the galaxy correlation

- Due to neutrio free streaming, the power spectrum of cosmological perturbations will be suppressed on scales smaller than

$$k_{nr} \approx 0.026 \left(\frac{m_\nu}{1\mathrm{eV}}\right)^{1/2} \Omega_m^{1/2} h\mathrm{Mpc}^{-1}$$

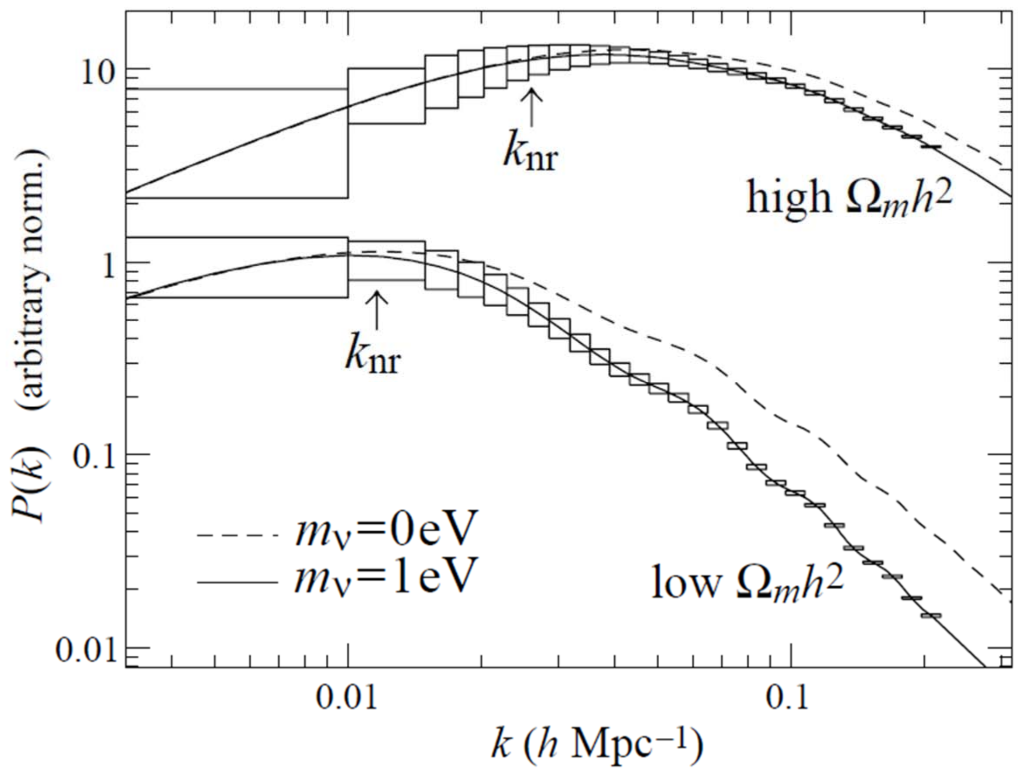

W. Hu, D. J. Eisenstein, and M. Tegmark, PRL80, 5255 (1998),

- W. Hu, D. J. Eisenstein, and M. Tegmark (1998) estimated this power suppression ratio to be

$$\frac{\Delta P}{P} \approx -8\frac{\Omega_\nu}{\Omega_m} \approx -0.8\left(\frac{m_\nu}{1\mathrm{eV}}\right)\left(\frac{0.1N}{\Omega_m h^2}\right)$$

- Because SDSS measures P with $\sim$ 1% accuracy at (0.1-0.2)h Mpc^{-1}, this implies that we can detect the neutrino mass larger than

$$m_{\min} \approx 0.02\left(\Omega_m h^2/0.1N\right)\mathrm{eV}$$

- However, due to degeneracies with other effects, only 50% accuracy can be achieved for m_ν by LRG power spectrum by SDSS

$$\sum m_\nu < 0.65\ (\Omega_m h^2/0.1N)^{0.8}\ \mathrm{eV}\ (2\sigma)$$

- Recently, this was applied to SDSS observations:

LRG power spectrum (SDSS (DR7)) on scales 0.02 < k < 0.2 h Mpc^{-1}

$\Rightarrow$ LCDM with $\Omega_m h^2(n_s/0.96)^{1.2}$ = *0.141+0.010−0.012* (prior: $\Omega_b h^2$ =0.02265)

+ WMAP5 (flat LCDM)

$\Rightarrow$ Ω_m =0.289$\pm$0.019, H_0 =69.4$\pm$1.6 kms^{-1} Mpc^{-1}.

$\Rightarrow$ $\sum m_\nu < 0.62$ eV or $N_{\nu\mathrm{eff}}$ = 3.2 – 6.4

[B. A. Reid, et al., MNRAS. 404, 60 (2010), 0907.1659]

Effective neutrino number

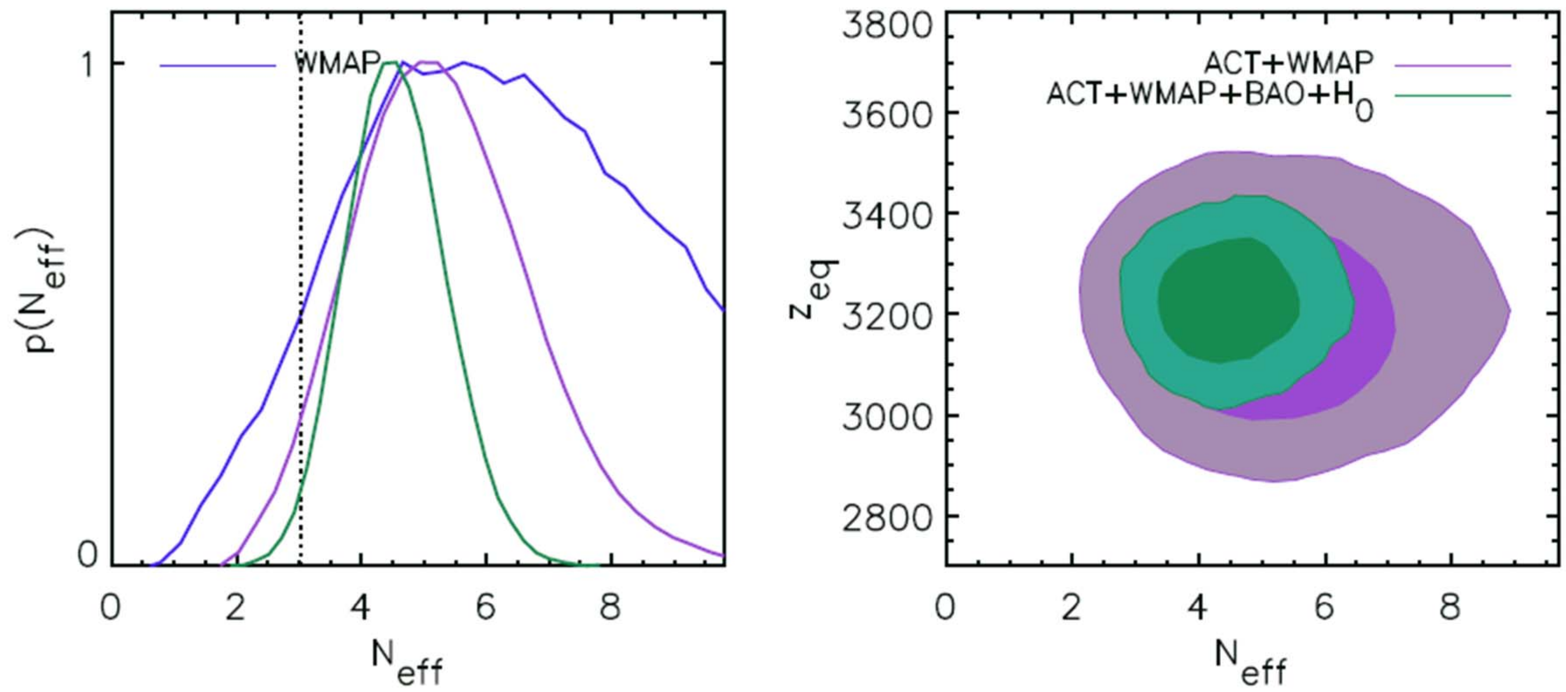

FIG. 9.— Constraints on the effective number of relativistic species, $N_{\rm eff}$. *Left*: One-dimensional marginalized distribution for $N_{\rm eff}$, for data combinations indicated in the right panel. The standard model assumes three light neutrino species ($N_{\rm eff}$=3.04, dotted line); the mean value is higher, but 3.04 is within the 95% CL. *Right:* Two-dimensional marginalized distribution for $N_{\rm eff}$ and equality redshift $z_{\rm eq}$, showing that $N_{\rm eff}$ can be measured separately from $z_{\rm eq}$. $N_{\rm eff}$ is bounded from above and below by combining the small-scale ACT measurements of the acoustic peaks with *WMAP* measurements. The limit is further tightened by adding BAO and H_0 constraints, breaking the degeneracy between $N_{\rm eff}$ and the matter density by measuring the expansion rate at late times.

Primordial Helium Abundance

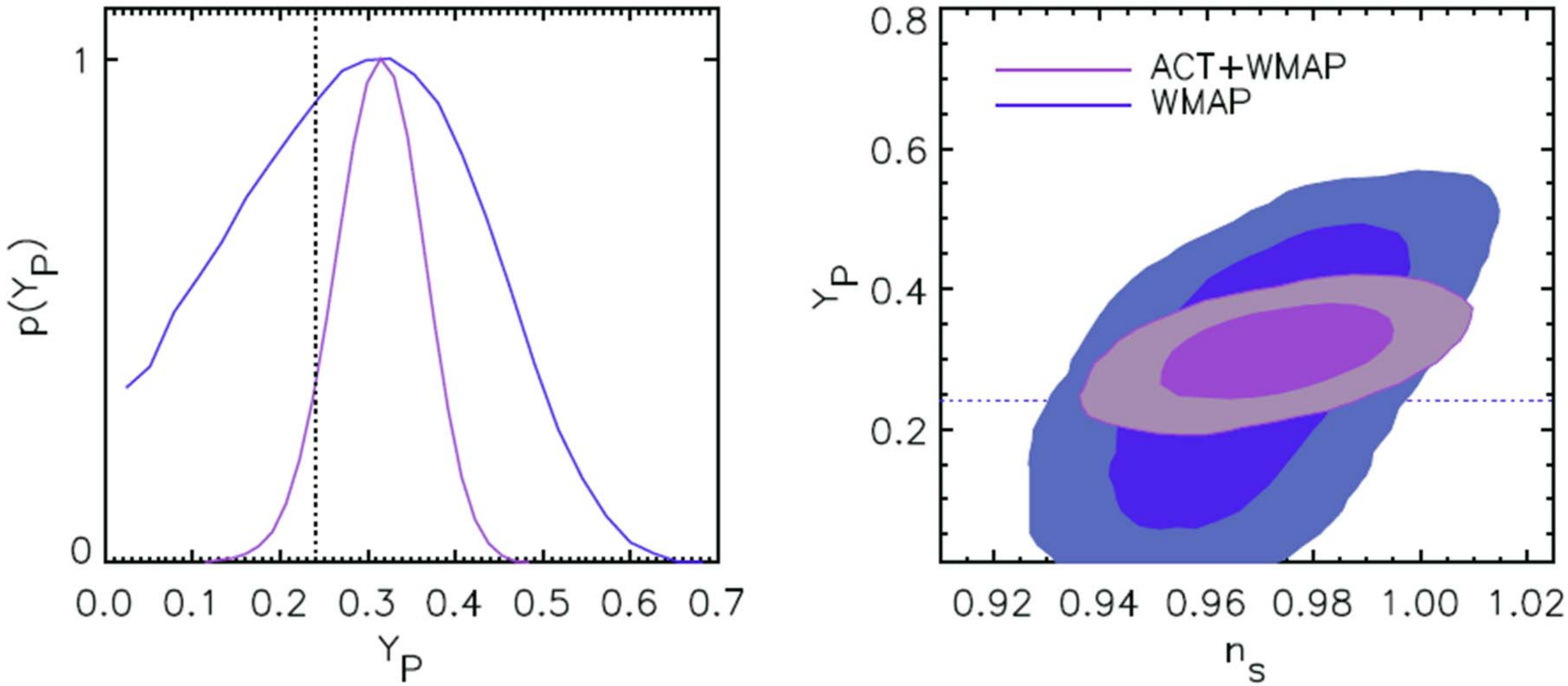

FIG. 10.— Constraint on the primordial helium mass fraction Y_P. *Left:* The one-dimensional marginalized distribution for Y_P derived from the ACT+*WMAP* data compared to *WMAP* alone. The measurement of the Silk damping tail by ACT constrains the number of free electrons at recombination, giving a 6σ detection of primordial helium consistent with the BBN-predicted $Y_P = 0.25$. *Right:* The two-dimensional marginalized distribution (68% and 95% CL) for Y_P and the spectral index n_s; the degeneracy is partly broken with the ACT data.

Cf: Y. I. Izotov, T. X. Thuan,:ApJ. 710, L67-L71 (2010).
Yp = 0.2565± 0.0010 (stat) ±0.0050 (syst)
Vs. WMAP Yp =0.2486 ± 0.0002 (68%CL)

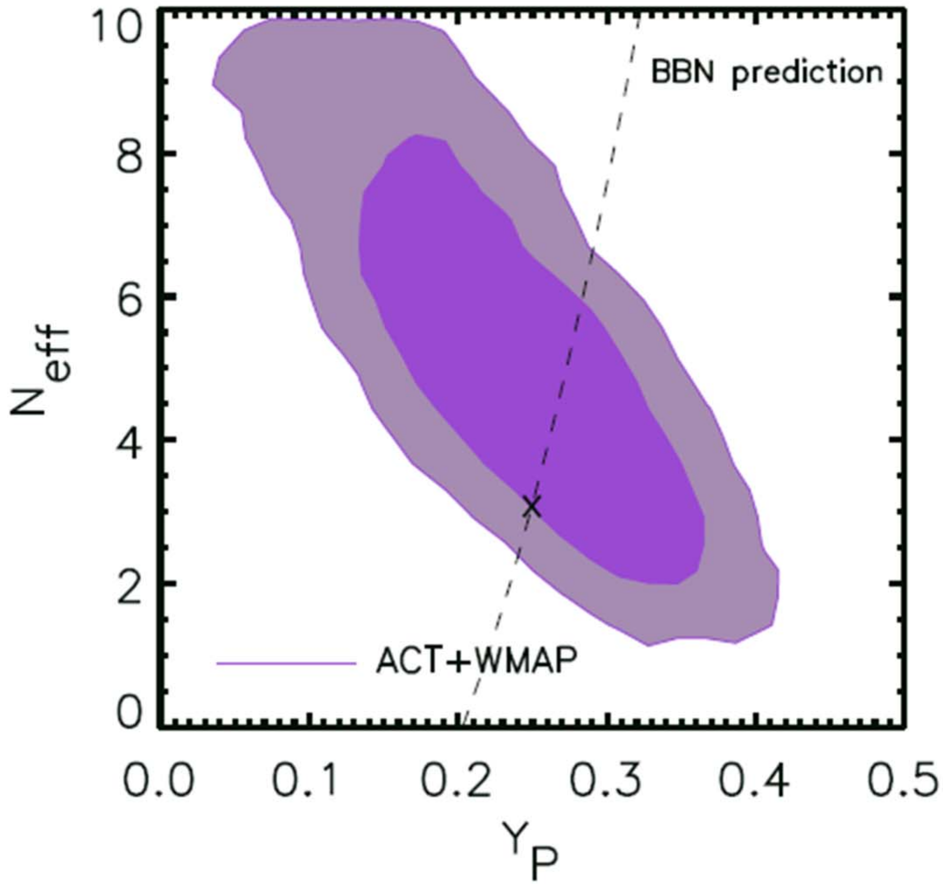

FIG. 11.— Joint two-dimensional marginalized distribution (68% and 95% CL) for the primordial helium mass fraction Y_P and the number of relativistic species $N_{\rm eff}$. The two are partly degenerate, as increasing $N_{\rm eff}$ or Y_P leads to increased damping of the power spectrum. The predicted standard-BBN relation between $N_{\rm eff}$ and Y_P is indicated. The concordance $N_{\rm eff}$=3.04, Y_P = 0.25 model lies on the edge of the two-dimensional 68% CL, and a model with $N_{\rm eff}$=0, Y_P = 0 is excluded at high significance.

FLUCTUATION OF AXION FIELDS

Perturbation Equations

Synchronous Gauge

$$ds^2 = a(\eta)^2 \left[-d\eta^2 + (g_{ij} + h_{ij})dx^i dx^j\right] \qquad \mathscr{H} := a'/a = aH$$

$$h_{ij}(\eta, x) = \int d^3k e^{ik\cdot x} \left[6H_L(\eta)\hat{k}_i\hat{k}_j - 2\mathscr{R}(\eta)(3\hat{k}_i\hat{k}_j - \delta_{ij})\right]$$

Einstein Equations

$$H_L'' + \mathscr{H} H_L' = -\frac{\kappa^2}{6} a^2 \left(\delta\rho + 3\delta P\right),$$

$$k^2\mathscr{R} + 3\mathscr{H} H_L' = \frac{\kappa^2}{2} a^2 \delta\rho$$

$$\delta\rho_a = \frac{1}{a^2}\phi_0'\phi_1' + m^2\phi_0\phi_1,$$

$$\delta P_a = \frac{1}{a^2}\phi_0'\phi_1' - m^2\phi_0\phi_1$$

Axion Field Equation

$$\phi(\eta, x) = \phi_0(\eta) + \phi_1(\eta, x)$$

$$\phi_1'' + 2\mathscr{H}\phi_1' + (m^2a^2 + k^2)\phi_1 = -3\phi_0' H_L'$$

Residual Gauge Freedom

Synchronous gauge + CDM comoving ⇒

$$\bar{\delta} H_L = \text{const}, \quad \bar{\delta}\mathscr{R} = 0,$$
$$\bar{\delta}\phi_1 = \bar{\delta}\rho = \bar{\delta}v = 0$$

Matter Perturbation Equations

Neglecting the baryon contribution,

$$\delta_c' = -3H_L',$$
$$\delta_\gamma' = -\frac{4}{3}\left(\theta_\gamma + 3H_L'\right),$$
$$\theta_\gamma' = \frac{1}{4}k^2\delta_\gamma$$

$$\delta = \delta\rho/\rho,$$
$$\theta = kv = \nabla \cdot \boldsymbol{v}$$

Initial Condition

Assumptions

Initially,

- Perturbations are adiabatic, and
- only growing modes exist.

Initial Condition

$$A = B = 0, \quad v_c = 0$$

$$H_L = C(k\eta)^2 + \mathrm{O}\big((k\eta)^4\big)\ ,$$
$$\mathscr{R} = -18C + \mathrm{O}\big((k\eta)^2\big)\ ,$$
$$\delta_c = \mathrm{O}\big((k\eta)^2\big)\ ,$$
$$\delta_\gamma = \mathrm{O}\big((k\eta)^2\big)\ ,$$
$$v_\gamma = \mathrm{O}\big((k\eta)^3\big)\ ,$$
$$\phi_1 = \mathrm{O}\big((k\eta)^2\big)$$

+ perturbation eqs

$$H_L = C(k)(k\eta)^2,$$
$$\delta_c = -3H_L,$$
$$\delta_\gamma = -4C(k)(k\eta)^2,$$
$$\theta_\gamma = -\frac{1}{3}C(k)k(k\eta)^3,$$
$$\phi_1 = \phi_1' = 0$$

Numerical Results

- They derived an empirical formula for the suppression factor S that coincides with that in the axiverse paper for small deformation

$$S(z) = \left[\frac{1+z}{(1+z_m)^{1.6}}\right]^{2r},$$

$$r \to \frac{3}{5}f; \quad f = \frac{\Omega_a}{\Omega_m} \to 0$$

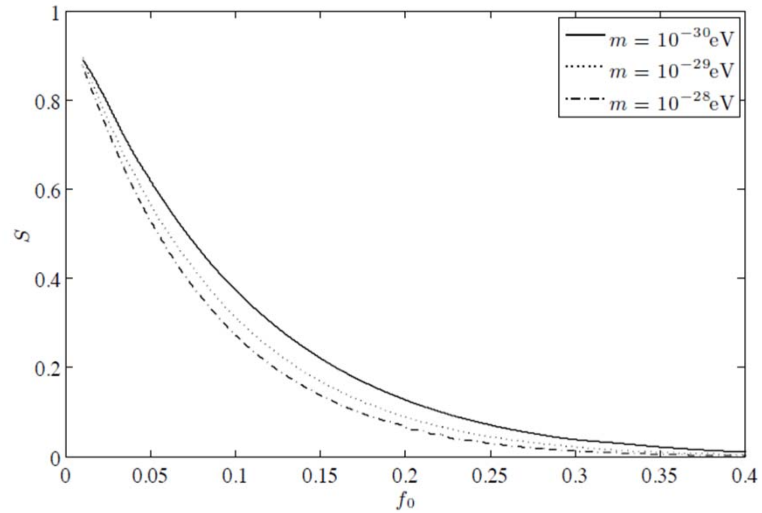

- They also obtained an empirical formula for the transition wave number consistent with the analytic estimate.

$$k_m \approx 1.25 f_0^{-0.5} m^{1/3} (1-\Omega_\Lambda)^{0.4}$$

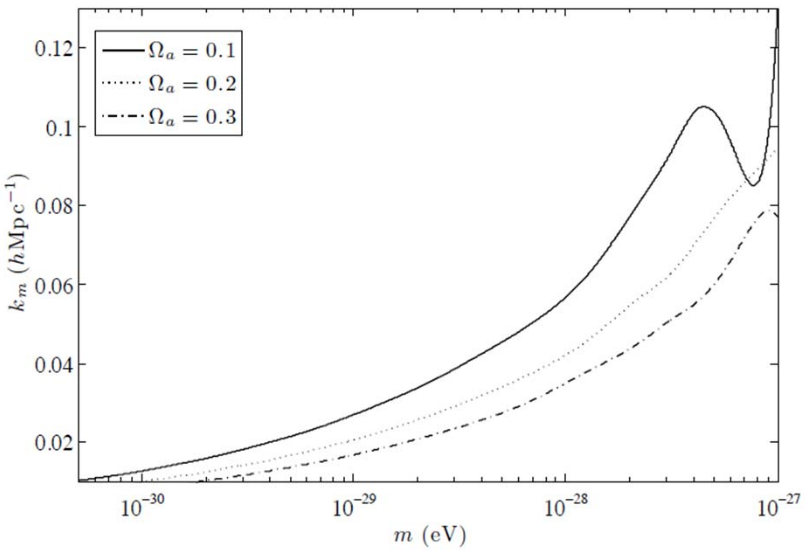

However, no oscillatory behavior appears in the transfer function!

Transfer function: $$T^2(k) := \frac{P(k)_{\mathrm{ALPs+CMD}}}{P(k)_{\mathrm{CMD}}}$$

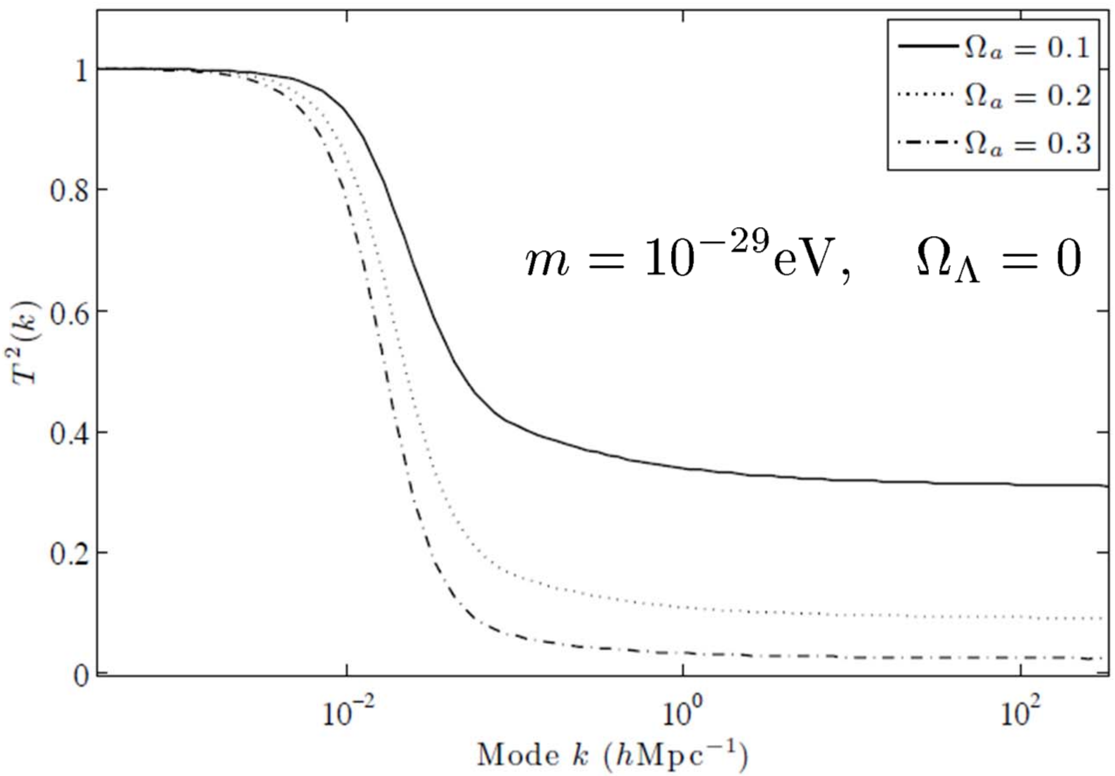

DISCUSSIONS

Are there axionic sound waves?

- The WKB analysis by W. Hu et al suggests that the concept of Jeans length L_J applies to axionic fields as well.
- The numerical calculation by Marsh and Ferreira shows that axionic perturbations damps when the perturbation scale becomes smaller than L_J.
- However, no oscillatory feature appears in the numerical result.

Numerical calculations are time-consuming.

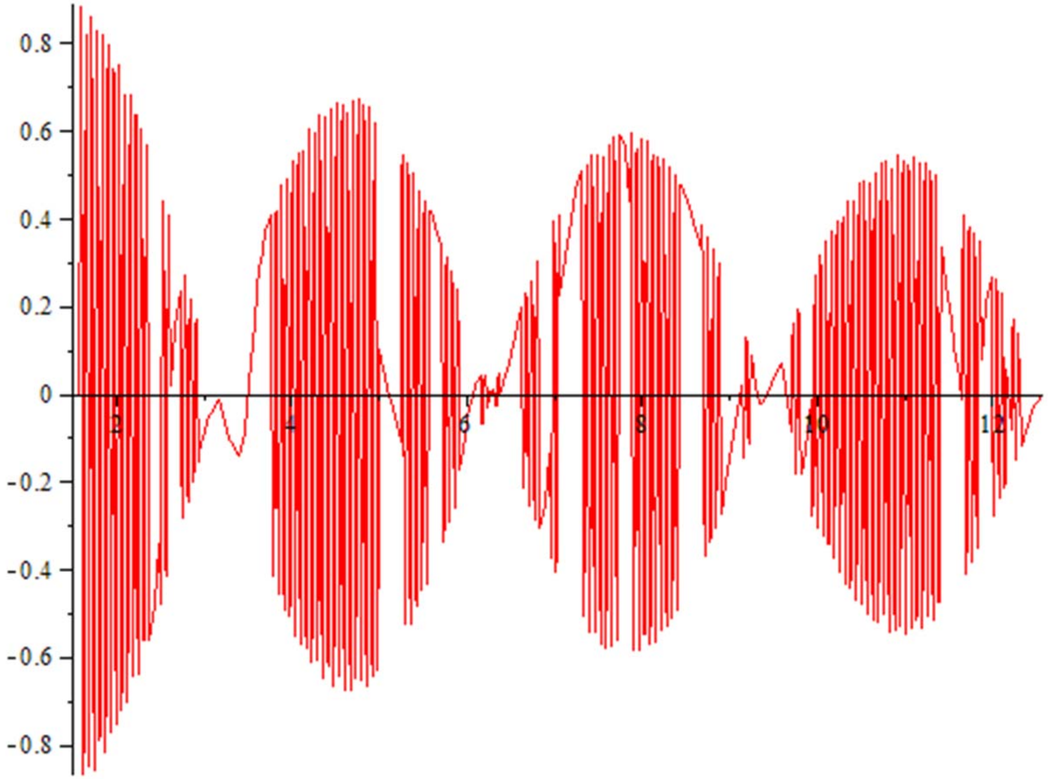

Analytic estimation is not easy.

- In the comoving synchronous gauge, the scalar field perturbation equation becomes 3-rd order even if we fix other matter perturbations.

$$\phi_1'' + 2\mathscr{H}\phi_1' + (m^2a^2 + k^2)\phi_1 = -3\phi_0' H_L'$$

$$(aH_L')' = -\frac{\kappa^2}{6}\left[4a\phi_0'\phi_1' - 2a^3m^2\phi_0\phi_1 + a^3(\delta\rho + 3\delta P)_m\right]$$

- In the standard gauge-invariant variables, the equation can be reduced to the 2nd-order, but the coefficient is singular around the wave number

$$\frac{k^2}{a^2} \sim \kappa^2\dot{\phi}^2$$

SUMMARY

Summary

- Superlight axions produced by string theory compactification can deform the power spectrum of large scale perturbations significantly.
- If the axion energy scale f_a is comparable to the GUT scale or larger, this deformation can be detected by future observations ($L \gtrsim 1$Mpc).
- In order to distinguish this deformation from similar effects caused by small neutrino masses, we have to study the fine structure of the transfer function more carefully.